Monthly Notices
of the
ROYAL ASTRONOMICAL SOCIETY

MNRAS **476,** 1835–1839 (2018)
Advance Access publication 2018 February 9

doi:10.1093/mnras/sty352

Resolving the host galaxy of a distant blazar with LBT/LUCI 1 + ARGOS

E. P. Farina,[1]★ I. Y. Georgiev,[1] R. Decarli,[1,2] T. Terzić,[3] L. Busoni,[4] W. Gässler,[1] T. Mazzoni,[4] J. Borelli,[1] M. Rosensteiner,[5] J. Ziegleder,[5] M. Bonaglia,[4] S. Rabien,[5] P. Buschkamp,[6] G. Orban de Xivry,[5] G. Rahmer,[7] M. Kulas[1] and D. Peter[1,8]

[1]*Max Planck Institut für Astronomie, Königstuhl 17, D-69117 Heidelberg, Germany*
[2]*Osservatorio Astronomico di Bologna, via Gobetti 93/3, I–40129 Bologna, Italy*
[3]*Department of Physics, University of Rijeka, Radmile Matejčić 2, HR-51000 Rijeka, Croatia*
[4]*Osservatorio Astrofisico di Arcetri, Largo Enrico Fermi 5, I-50125 Florence, Italy*
[5]*Max Planck Institut für Extraterrestrische Physik, Giessenbachstrasse 1, D-85748 Garching, Germany*
[6]*Buschkamp Research Instruments, Elisabethstrasse 2, D-80796 München, Germany*
[7]*LBT Observatory, University of Arizona, 933 N. Cherry Ave, Tucson, AZ-85721, USA*
[8]*Heidelberg Instruments Mikrotechnik GmbH, Tullastrasse 2, D-69126 Heidelberg, Germany*

Accepted 2018 January 18. Received 2018 January 15; in original form 2017 October 14

ABSTRACT

BL Lac objects emitting in the very high energy (VHE) regime are unique tools to peer into the properties of the extragalactic background light (EBL). However, due to the typical absence of features in their spectra, the determination of their redshifts has proven challenging. In this work, we exploit the superb spatial resolution delivered by the new Advanced Rayleigh guided Ground layer adaptive Optics System (*ARGOS*) at the Large Binocular Telescope to detect the host galaxy of HESS J1943+213, a VHE emitting BL Lac shining through the Galaxy. Deep *H*-band imaging collected during the ARGOS commissioning allowed us to separate the contribution of the nuclear emission and to unveil the properties of the host galaxy with unprecedented detail. The host galaxy is well fitted by a Sérsic profile with index of $n \sim 2$ and total magnitude of $H_{\rm Host} \sim 16.15$ mag. Under the assumption that BL Lac host galaxies are standard candles, we infer a redshift of $z \sim 0.21$. In the framework of the current model for the EBL, this value is in agreement with the observed dimming of the VHE spectrum due to the annihilation of energetic photons on the EBL

Key words: instrumentation: adaptive optics – BL Lacertae objects: individual: HESS J1943+213 – infrared: galaxies.

1 INTRODUCTION

In the classical unified model, blazars constitute a class of active galactic nuclei (AGNs) viewed at small angles from the jet axis (Blandford & Rees 1978; Antonucci 1993; Urry & Padovani 1995). Traditionally, blazars have been further splitted into two subclasses based on the strength of the features present in their optical spectra. While flat-spectrum radio quasars (FSRQs) show emission lines with equivalent width $\gtrsim$5 Å, in BL Lacertae objects (BL Lacs) the non-thermal synchrotron radiation of the jet completely dominates the optical/UV emission, ending up in a typical featureless power-law spectrum. This makes the determination of their redshift via the detection of absorption/emission lines from the nuclear emission and/or from the host galaxy particularly challenging, even with 8–10 m class telescopes (e.g. Sbarufatti et al. 2005a, 2006, 2009; Landoni et al. 2013; Sandrinelli et al. 2013; Shaw et al. 2013; Falomo, Pian & Treves 2014; Pita et al. 2014; Paiano et al. 2016; Rosa-Gonzalez et al. 2017 for a review). In past years, several alternatives have been proposed to constrain the redshift of BL Lac objects, including the detection of intervening absorption features either from the halo of lower redshift galaxies (e.g. Shaw et al. 2013; Landoni et al. 2014) or from the neutral hydrogen in the intergalactic medium (e.g. Danforth et al. 2010; Furniss et al. 2013); the spectroscopy of galaxies in the environment where the blazars are embedded (e.g. Muriel et al. 2015; Farina et al. 2016); the detection of molecular emission lines from the host galaxy (e.g. Fumagalli et al. 2012); the study of the effect of the interaction with the extragalactic background light (EBL) in the blazar emission in the GeV and TeV domain (e.g. Prandini et al. 2010; Prandini, Bonnoli & Tavecchio 2012). In particular, the narrow distribution in luminosity of BL Lac host galaxies (Urry et al. 2000; Sbarufatti, Treves & Falomo 2005b) opened the possibility to use them as standard candles, and thus to measure their distance via broad-band imaging

★ E-mail: emanuele.paolo.farina@gmail.com

(e.g. Nilsson et al. 2008; Meisner & Romani 2010; Kotilainen et al. 2011). The main challenge of this approach is to accurately remove the bright central emission that typically outshine the host galaxy. Given the average 1.0 arcsec (or 3.2 kpc in the considered cosmology) effective radius calculated from the collection of $z \lesssim 0.6$ BL Lac hosts observed with *HST* by Scarpa et al. (2000), it is clear that images with an exquisite spatial resolution and high contrast are necessary to unveil the faint and diffuse starlight emission around the bright, point-like emission from the active nucleus. In this paper, we exploit the capabilities of the new Advanced Rayleigh guided Ground layer adaptive Optics System (*ARGOS*; Rabien et al. 2010) mounted on the Large Binocular Telescope (LBT; Hill & Salinari 2004; Hill et al. 2012) to collect high-resolution near-infrared (NIR) LUCI 1 (i.e. LBT Utility Camera in the Infrared; Seifert et al. 2003; Ageorges et al. 2010) observations of HESS J1943+213. This blazar was detected by *HESS* in the very high energy (VHE) domain (i.e. at $E > 100$ GeV) during a VHE galactic survey (H.E.S.S. Collaboration et al. 2011), making it the only BL Lac object known located in the Galactic plane. Broad *Ks*-band images gathered with the 3.5 m CAHA telescope revealed the presence of an extended emission that has been attributed to the host galaxy of HESS J1943+21 (Peter et al. 2014). A comparison with the typical size of blazar host derived by Cheung et al. (2003) allowed Peter et al. (2014) to set a lower limit on the redshift of $z > 0.03$. This is consistent with the $z > 0.14$ derived from the fit of the spectral energy distribution of HESS J1943+21 (Cerruti 2011; H.E.S.S. Collaboration et al. 2011) and with the $z < 0.45$ limit obtained via modelling the attenuation of the VHE emission by the EBL (Peter et al. 2014). A tighter constraint on the redshift is however necessary to understand the nature of the VHE emission and to derive the EBL properties.

Throughout this paper, we assume a concordance cosmology with $H_0 = 70\,\mathrm{km\,s^{-1}\,Mpc^{-1}}$, $\Omega_\mathrm{m} = 0.3$, and $\Omega_\Lambda = 0.7$. All the quoted magnitudes are expressed in the AB standard photometric system (Oke 1974; Oke & Gunn 1983).

2 OBSERVATIONS AND DATA REDUCTION

NIR data in the *H* band with the LBT/LUCI 1 NIR camera were collected during the ARGOS commissioning run on 2016-10-20. ARGOS uses a natural guide star (NGS) for guiding, while three green light (532 nm) lasers focused at 12 km (the laser guide stars, LGSs) are used to correct for the ground layer turbulence. The LGSs are situated on a circle with radius 2 arcmin that provides adaptive optics (AO) correction across the entire 4 arcmin×4 arcmin LUCI 1 field of view (see Fig. 1). The NGS that we used is conveniently bright for guiding (R=16.5 mag) but too faint for fast wave front sensing without the lasers. The location of the NGS was close ($\Delta r =$ 5 arcsec) to our target and it was placed in the centre of the LUCI 1 field. This provides an excellent condition for the optimal ARGOS AO performance and stability of the point spread function (PSF; see Section 3). Naturally, the seeing in the optical is higher than that in the NIR and during the night it was around 1.0 ± 0.1 arcsec, while that in the *H* band was around 0.45 ± 0.05 arcsec. The use of ARGOS halved the natural seeing in the *H* band to 0.26 arcsec (FWHM = 2.2 pixel). To obtain good sky subtraction, we used a 30 arcsec×30 arcsec dither box. This is significantly larger (>5×) than the angular size of our target and accounts also for the nearby bright foreground star. Each offset and exposure acquisition was completed to within 1 min, which allowed to combine five offsets and map well the temporal variation of the NIR night sky. Data reduction was performed within the IRAF environment. Master dark and flat-field calibration data were used to reduce the raw images.

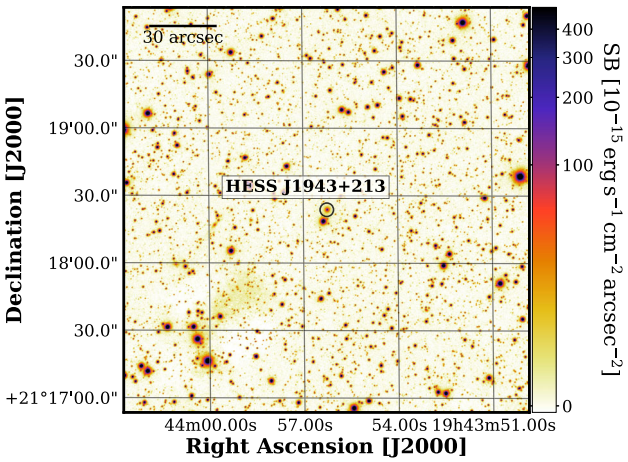

Figure 1. The central 3 arcmin×3 arcmin region around HESS J1943+213 as imaged in the *H* Band with LBT/LUCI 1+ARGOS (north is up and west is to the right). Marked with a circle is the position of the blazar (corresponding to the source located at R.A.$_{\mathrm{J2000}}$ = 19:43:57.63 and Dec.$_{\mathrm{J2000}}$ = +21:18:31.5 in the 2MASS catalogue; Cutri et al. 2003). The large field of view of LBT/LUCI 1+ARGOS and the location of the source close to the Galactic plane (with Galactic latitude $b = -1.^\circ2947$) allowed us to sample well and build good PSF model (see Section 3).

Correction for persistence and non-linearity was performed using pixel maps as described in Georgiev et al. (in preparation). In total, we combined 228 individual exposures, each of DIT = 2.8 s. The short DIT was required to avoid badly saturating foreground stars and avoiding strong persistence. The final image registration and combination were performed with our custom wrapper routine built around the main IRAF tasks *geomap, geotran, imcombine*. During the final geometric image transformation and combination, we used a drizzle drop fraction of 0.8 and a 20×20 pixels statistics region to check additionally for residual background variation between the individual exposures.

The resulting image[1] (see Fig. 1) was then WCS registered using the ASTROMETRY.NET tool (Lang et al. 2010) and calibrated in flux matching sources detected in the field with the 2MASS catalogue (Cutri et al. 2003). We adopted the conversion from Vega to AB magnitudes from Blanton et al. (2005). Uncertainties in the zero-point are of the order of 0.06 mag. The 5σ detection limit for a point source (estimated from the rms of the sky counts integrated over the radius of an unresolved source, i.e. 1.1 pixel) is $H_\mathrm{lim} \approx$ 23.5 mag. We consider the reddening correction from Schlafly & Finkbeiner (2011) [$E(B-V) = 2.30$ mag, towards the location of the blazar]. Assuming a visual extinction to reddening ratio of $R_V = A_V/E(B-V) = 3.1$ (e.g. Cardelli, Clayton & Mathis 1989; Fitzpatrick 1999) and the Cardelli et al. (1989) extinction curve, this corresponds to an *H*-band extinction of $A_H^c = 1.30$ mag. The dust extinction in this region of the Galaxy, however, is not well constrained. For instance, a much lower extinction [$E(B-V) =$ 1.76 mag] is reported by Green et al. (2015) for the same region of the sky. In the following, we thus consider that the *H*-band extinction can vary from $A^c_{H,\mathrm{min}} = 1.19$ mag and $A^c_{H,\mathrm{Max}} = 1.62$ mag, corresponding, respectively, to the minimum and maximum values of $E(B-V)$ observed within a circle of 5 arcmin radius centred at the location of HESS J1943+213 (Schlafly & Finkbeiner 2011).

[1] The reduced image is publicly available at https://github. com /EmAstro/LBT_ARGOS

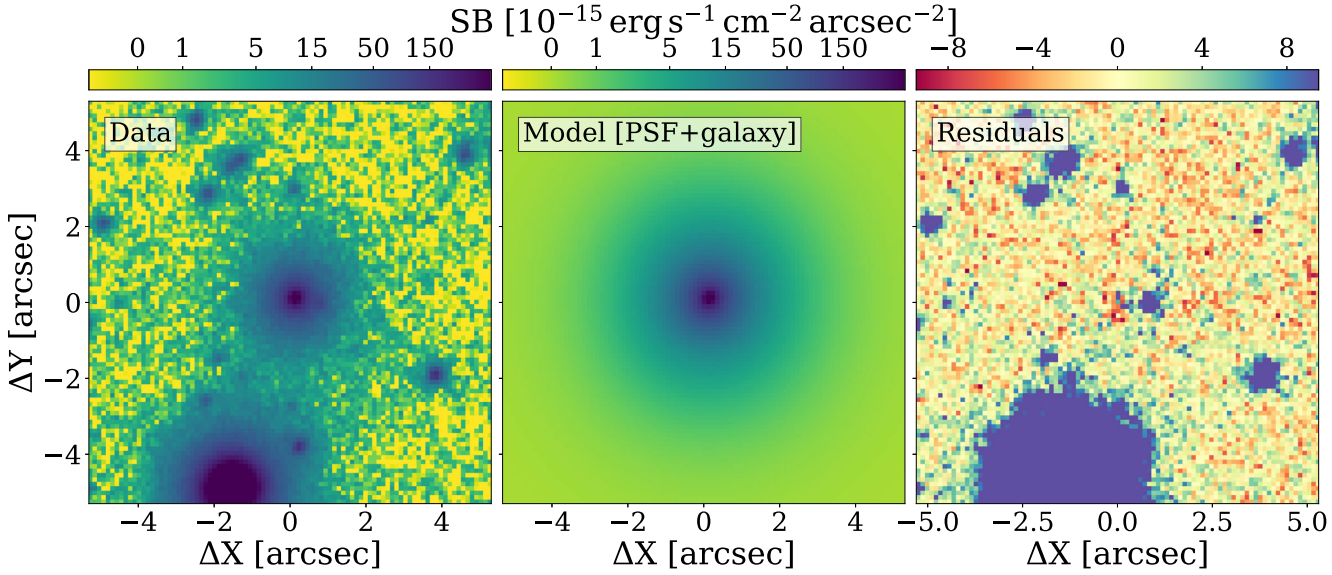

Figure 2. Results from the point source and host galaxy modelling of the blazar HESS J1943+213. Left: thumbnail of the LBT/LUCI 1+ARGOS *H*-band image centred at the blazar location. For display purposes, the best fit of the background provided by GALFIT has been removed. In all panels, north is up and west is right. Central: the best-fitting GALFIT model. The PSF model was created as described in Section 3. The host galaxy light appears to follow a Sérsic profile with index $n = 2.2$ and effective radius $R_e \sim 1.1$ arcsec. The derived total magnitude of the host galaxy is: $H_{Host} = 16.15$ mag (not corrected for Galactic extinction). An independent analysis performed with IMFIT results in a similar solution for the fit. Right: residuals after model subtraction. The residual image shows a source located at 0.6 arcsec west from the centre of the blazar. We masked it during the fitting process in order to avoid contaminating the extended emission from the host galaxy.

3 SUBTRACTION OF THE PSF

The model of the PSF was built by using 68 Milky Way foreground stars. They were chosen to have no contamination from neighbours within the radius of the PSF model, to sample well the detector and build a spatially variable PSF. As mentioned in Section 2, the NGS is projected very close to our blazar and is in the centre of the LUCI 1 field. This guarantees a very stable and sharp PSF, although, as shown in Georgiev et al. (in preparation), its global variation is up to 25 per cent towards the detector edges.

This PSF model was then ingested into GALFIT (version 3.0.5; Peng et al. 2010) in order to infer the properties of the extended emission around HESS J1943+213. To avoid contamination from nearby objects, we masked all sources present within a 10 arcsec radius from the blazar, including the faint, unresolved object located 0.6 west from HESS J1943+213 (see Fig. 2). As a first step, we assumed the source as unresolved. In this case, the entire emission would fall within our PSF model. The fit of a pure PSF (representing the central, unresolved nuclear emission) and of the sky background leave, however, significant residuals, confirming the presence of an extended emission (see Fig. 3). In addition to the PSF model and to the sky emission, we thus simultaneously fitted a galaxy component modelled with a Sérsic profile (Sérsic 1963). This second approach leaves only negligible residuals. Results of the fitting procedure are shown in Figs 2 and 3 and summarized in Table 1.

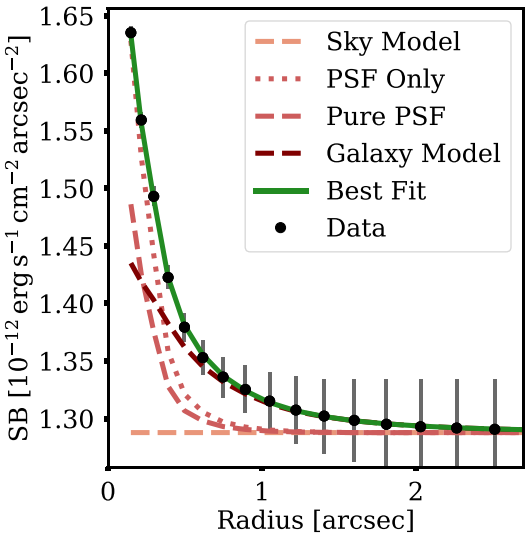

Figure 3. Radial intensity profile of the BL Lac emission extracted in circular annulii (black points). The different components used to model the emission of HESS J1943+213 are marked with different coloured dashed lines (see Fig. 2 and Section 3). The total fit is shown as a green solid line. The dotted line illustrates the result of the fitting procedure assuming that no extended emission is present in the data. It is evident that the host galaxy emission is much more extended than the PSF.

4 PROPERTIES OF THE HOST GALAXY

Table 1 summarizes the results of our fit. The nuclear (unresolved) emission is $H_{PSF} = 18.10$ mag, while the host galaxy appears to be brighter with $H_{Host} = 16.15$ mag. The derived values for the effective radius ($R_e = 1.13$ arcsec) and for the Sérsic index ($n = 2.20$) are in contrast with the 2.0 arcsec $\lesssim R_e \lesssim$ 2.5 arcsec and $n \sim 8$ estimated by Peter et al. (2014). These were derived from the analysis of a *Ks*-band image collected with the wide field camera OMEGA2000 on the 3.5 m Calar Alto telescope. The smaller values we recover for both R_e and n are consistent with an independent analysis performed with the IMFIT package (Erwin 2015), where instead of masking it, we also fit for the source (star) projected close to the blazar. We argue that the discrepancies between the Peter et al. (2014) and our study are due to the much higher spatial

Table 1. Result from the GALFIT fit of the blazar HESS J1943+213. Magnitudes are not corrected for Galaxy extinction.

Parameter	Value
$H_{\rm PSF}$	$\left(18.10^{+0.07}_{-0.05}\right)$ mag
$H_{\rm Host}$	$\left(16.15^{+0.01}_{-0.03}\right)$ mag
$R_{\rm e}$	$\left(1.13^{+0.02}_{-0.04}\right)$ arcsec
Sérsic index	$\left(2.20^{+0.31}_{-0.23}\right)$
Axis ratio	$\left(0.92^{+0.01}_{-0.01}\right)$
Position angle	$\left(-1.^{\circ}49^{+0.^{\circ}12}_{-3.^{\circ}73}\right)$

resolution delivered by ARGOS. [2] In addition, Peter et al. (2014) model the blazar emission with a single Sérsic profile (i.e. without removing the PSF). An underestimate of the contribution from the nuclear emission may explain the high Sérsic index observed in the OMEGA2000 image.

Given the magnitude of the host galaxy, we can now estimate the redshift of HESS J1943+213, using the typical absolute magnitude of BL Lac host galaxies as a standard candle. Indeed, Sbarufatti, Treves & Falomo (2005b) showed that, at $z < 0.7$, the distribution of the rest-frame *R*-band absolute magnitude of BL Lac host galaxies is almost Gaussian, with an average of $\langle {\rm M_R} \rangle = -22.6$ and standard deviation $\sigma_{\rm M_R} = 0.5$. To translate, as a function of redshift, the observed *H*-band apparent magnitude into an *R*-band absolute magnitude, we considered the Mannucci et al. (2001) elliptical galaxy template and a passive evolution of the stellar population (Bressan, Granato & Silva 1998). This allowed us to find at which redshift the observed magnitude of the host galaxy match $\langle {\rm M_R} \rangle = -22.6$. Assuming $A^c_{\rm H} = 1.30$ mag, we derive a redshift $z = 0.21$ (varying from $z = 0.17$ to 0.28 for $\langle {\rm M_R} \rangle - \sigma_{\rm M_R}$ and $\langle {\rm M_R} \rangle + \sigma_{\rm M_R}$, respectively). At this redshift, the physical effective radius of the host galaxy is $R_{\rm e} = 3.9$ kpc. We also took into account the effects of the uncertainties in the Galactic extinction presented in Section 2. These led to slightly different results, ranging from $z = 0.23$ for $A^c_H = 1.19$ mag to $z = 0.18$ for $A^c_H = 1.62$ mag (see Fig. 4).

5 SUMMARY AND CONCLUSIONS

We obtained deep LBT/LUCI 1 *H*-band imaging of the blazar HESS J1943+213 detected by *HESS* in the VHE domain. The superb spatial resolution (FWHM = 0.26 arcsec) delivered by the new AO system, ARGOS, allowed us to precisely separate the unresolved nuclear component from the extended host galaxy emission.

The host galaxy of HESS J1943+213 appears round (with an axis ratio of ∼0.92), with a Sérsic index $n \sim 2.2$, and with *H*-band magnitude of $H_{\rm Host} \sim 16.15$ mag. Assuming the host galaxy as a standard candel, we locate HESS J1943+213 at $z \sim 0.21$, or, more conservatively, in the redshift range $0.14 < z < 0.30$ (considering variation of the typical luminosity of BL Lac host galaxies and uncertainties in the Galactic extinction). This range is consistent with the limits set by comparing measured spectra in high energy (HE, $E < 100$ GeV) and VHE ($E > 100$ GeV) ranges (see e.g. Stecker, Scully & Malkan 2016). Assuming any difference between the two was a consequence of absorption of the VHE γ-rays by the EBL, Peter et al. (2014) were able to set the upper limit to $z < 0.45$, with the most likely value of $z = 0.22$. Our result agrees very well with their estimate, and our upper limit of $z < 0.30$ is well below the one set by Peter et al. (2014). The spectra measured by *VERITAS* (Shahinyan 2017) in the 2014–2015 period are slightly harder, although consistent with *HESS* measurements. Therefore, the extrapolated and EBL-attenuated *Fermi*-LAT spectrum should also fit *VERITAS* spectral points. Despite the fact that we set the most stringent limits on redshift up to date, the uncertainties are still rather high, allowing for the measured VHE spectra to be a result of combination of intrinsic spectral features and the EBL absorption.

In addition, we detect a source located only 0.6 arcsec west from the BL Lac. Although it is very likely a foreground star, if it is at the same redshift as HESS J1943+213, this corresponds to a physical distance of ∼2.1 kpc. This may be suggestive for a rich environment, as commonly observed around other BL Lac host galaxies (e.g. Muriel 2016).

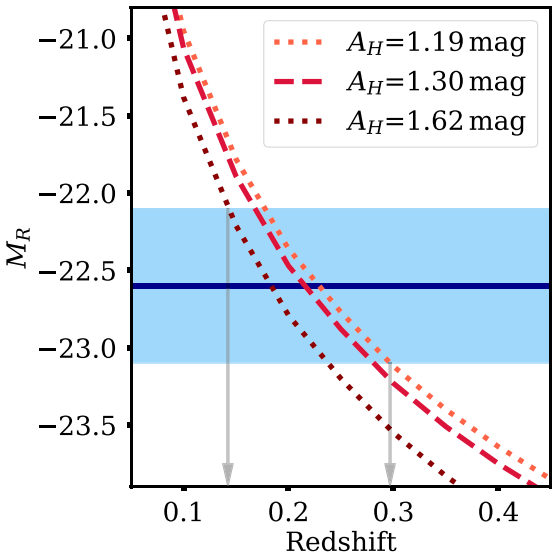

Figure 4. Expected rest-frame *R*-band absolute magnitude of the host galaxy HESS J1943+213 as a function of redshift (see Section 4 for details). Dashed and dotted lines show the effect of a different level of dust extinction. The average M_R of BL Lac host galaxies derived by Sbarufatti, Treves & Falomo (2005b) is shown as a horizontal blue line, with the $\pm 1\sigma$ regime highlighted in light blue. The redshift of HESS J1943+213 is thus constrained in the range $0.14 \lesssim z \lesssim 0.30$ (vertical grey arrows).

ACKNOWLEDGEMENTS

EPF acknowledges funding through the ERC grant 'Cosmic Dawn'. EPF is grateful to T. A. Gutcke for introducing and providing support for an efficient use of PYTHON and of JUPYTER NOTEBOOK for analysing and plotting the data. This research made use of ASTROPY, a community-developed core PYTHON package for Astronomy (Astropy Collaboration et al. 2013), of APLPY,[3] an open-source plotting package for PYTHON based on MATPLOTLIB (Hunter 2007), and of IRAF.[4] Based on observations collected at the LBT, the LBT is an

[2] Seeing during the observations of HESS J1943+213 at Calar Alto was between 1.1 and 1.6 arcsec.

[3] http://aplpy.github.io/

[4] IRAF (Tody 1986, 1993) is distributed by the National Optical Astronomy Observatories, which are operated by the Association of Universities for Research in Astronomy, Inc., under cooperative agreement with the National Science Foundation.

international collaboration among institutions in the United States, Italy, and Germany. LBT Corporation partners are: The University of Arizona on behalf of the Arizona Board of Regents; Istituto Nazionale di Astrofisica, Italy; LBT Beteiligungsgesellschaft, Germany, representing the Max-Planck Society, The Leibniz Institute for Astrophysics Potsdam, and Heidelberg University; The Ohio State University, and The Research Corporation, on behalf of The University of Notre Dame, University of Minnesota and University of Virginia.

REFERENCES

Ageorges N. et al., 2010, in McLean I. S., Ramsay S. K., Takami H., eds, Proc. SPIE Conf. Ser. Vol. 7735, Ground-based and Airborne Instrumentation for Astronomy III. SPIE, Bellingham, p. 77351L
Antonucci R., 1993, ARA&A, 31, 473
Astropy Collaboration et al., 2013, A&A, 558, A33
Blandford R. D., Rees M. J., 1978, in Wolfe A. M., ed., Pittsburgh Conference on BL Lac Objects. p. 328
Blanton M. R. et al., 2005, AJ, 129, 2562
Bressan A., Granato G. L., Silva L., 1998, A&A, 332, 135
Cardelli J. A., Clayton G. C., Mathis J. S., 1989, ApJ, 345, 245
Cerruti M., 2011, Int. Cosmic Ray Conf., 8, 109
Cheung C. C., Urry C. M., Scarpa R., Giavalisco M., 2003, ApJ, 599, 155
Cutri R. M. et al., 2003, VizieR Online Data Catalog, 2246
Danforth C. W., Keeney B. A., Stocke J. T., Shull J. M., Yao Y., 2010, ApJ, 720, 976
Erwin P., 2015, ApJ, 799, 226
Falomo R., Pian E., Treves A., 2014, A&AR, 22, 73
Farina E. P., Fumagalli M., Decarli R., Fanidakis N., 2016, MNRAS, 455, 618
Fitzpatrick E. L., 1999, PASP, 111, 63
Fumagalli M., Dessauges-Zavadsky M., Furniss A., Prochaska J. X., Williams D. A., Kaplan K., Hogan M., 2012, MNRAS, 424, 2276
Furniss A. et al., 2013, ApJ, 768, L31
Green G. M. et al., 2015, ApJ, 810, 25
H. E. S. S. Collaboration et al. 2011, A&A, 529, A49
Hill J. M., Salinari P., 2004, in Oschmann J. M., Jr, ed., Proc. SPIE Conf. Ser. Vol. 4477, Astronomical Data Analysis. SPIE, Bellingham, p. 603
Hill J. M., Green R. F., Ashby D. S., Brynnel J. G., Cushing N. J., Little J. K., Slagle J. H., Wagner R. M., 2012, in Stepp L. M., Gilmozzi R., Hall H. J., eds, Proc. SPIE Conf. Ser. Vol. 8444, Ground-based and Airborne Telescopes IV. SPIE, Bellingham, p. 84441A
Hunter J. D., 2007, Comput. Sci. Eng., 9
Kotilainen J. K., Hyvönen T., Falomo R., Treves A., Uslenghi M., 2011, A&A, 534, L2
Landoni M., Falomo R., Treves A., Sbarufatti B., Barattini M., Decarli R., Kotilainen J., 2013, AJ, 145, 114
Landoni M., Falomo R., Treves A., Sbarufatti B., 2014, A&A, 570, A126
Lang D., Hogg D. W., Mierle K., Blanton M., Roweis S., 2010, AJ, 139, 1782
Mannucci F., Basile F., Poggianti B. M., Cimatti A., Daddi E., Pozzetti L., Vanzi L., 2001, MNRAS, 326, 745
Meisner A. M., Romani R. W., 2010, ApJ, 712, 14
Muriel H., 2016, A&A, 591, L4
Muriel H., Donzelli C., Rovero A. C., Pichel A., 2015, A&A, 574, A101
Nilsson K., Pursimo T., Sillanpää A., Takalo L. O., Lindfors E., 2008, A&A, 487, L29
Oke J. B., 1974, ApJS, 27, 21
Oke J. B., Gunn J. E., 1983, ApJ, 266, 713
Paiano S., Landoni M., Falomo R., Scarpa R., Treves A., 2016, MNRAS, 458, 2836
Peng C. Y., Ho L. C., Impey C. D., Rix H.-W., 2010, AJ, 139, 2097
Peter D., Domainko W., Sanchez D. A., van der Wel A., Gässler W., 2014, A&A, 571, A41
Pita S. et al., 2014, A&A, 565, A12
Prandini E., Bonnoli G., Maraschi L., Mariotti M., Tavecchio F., 2010, MNRAS, 405, L76
Prandini E., Bonnoli G., Tavecchio F., 2012, A&A, 543, A111
Rabien S. et al., 2010, in Ellerbroek B. L., Hart M., Hubin N., Wizinowich P. L., eds, Proc. SPIE Conf. Ser. Vol. 7736, Adaptive Optics Systems II. SPIE, Bellingham, p. 77360E
Rosa-Gonzalez D. et al., 2017, MNRAS, 466, 540
Sandrinelli A., Treves A., Falomo R., Farina E. P., Foschini L., Landoni M., Sbarufatti B., 2013, AJ, 146, 163
Sbarufatti B., Treves A., Falomo R., Heidt J., Kotilainen J., Scarpa R., 2005a, AJ, 129, 559
Sbarufatti B., Treves A., Falomo R., 2005b, ApJ, 635, 173
Sbarufatti B., Treves A., Falomo R., Heidt J., Kotilainen J., Scarpa R., 2006, AJ, 132, 1
Sbarufatti B., Ciprini S., Kotilainen J., Decarli R., Treves A., Veronesi A., Falomo R., 2009, AJ, 137, 337
Scarpa R., Urry C. M., Falomo R., Pesce J. E., Treves A., 2000, ApJ, 532, 740
Schlafly E. F., Finkbeiner D. P., 2011, ApJ, 737, 103
Seifert W. et al., 2003, in Iye M., Moorwood A. F. M., eds, Proc. SPIE Conf. Ser. Vol. 4841, Instrument Design and Performance for Optical/Infrared Ground-based Telescopes. SPIE, Bellingham, p. 962
Sérsic J. L., 1963, Bol. Asoc. Argentina Astron., 6, 41
Shahinyan K., 2017, AIP Conf. Ser. Vol. 1792, 6th International Symposium on High Energy Gamma-Ray Astronomy. Am. Inst. Phys., New York, p. 040036
Stecker F. W., Scully S. T., Malkan M. A., 2016, ApJ, 827, 6
Shaw M. S. et al., 2013, ApJ, 764, 135
Tody D., 1986, in Crawford D. L., ed., Proc. SPIE Conf. Ser. Vol. 627, Instrumentation in Astronomy VI. SPIE, Bellingham, p. 733
Tody D., 1993, in Hanisch R. J., Brissenden R. J. V., Barnes J., eds, ASP Conf. Ser. Vol. 52, Astronomical Data Analysis Software and Systems II. Astron. Soc. Pac., San Francisco, p. 173
Urry C. M., Padovani P., 1995, PASP, 107, 803
Urry C. M., Scarpa R., O'Dowd M., Falomo R., Pesce J. E., Treves A., 2000, ApJ, 532, 816

This paper has been typeset from a TEX/LATEX file prepared by the author.